Neurosci Bull June 1, 2012, 28(3): 209–221. http://www.neurosci.cn
DOI: 10.1007/s12264-012-1234-6

·Original Article·

Pharmacological kinetics of BmK AS, a sodium channel site 4-specific modulator on $Na_v1.3$

Zhi-Rui Liu[1], Jie Tao[1], Bang-Qian Dong[1], Gang Ding[2], Zhi-Jun Cheng[2], Hui-Qiong He[1,#], Yong-Hua Ji[1]

[1]*Laboratory of Neuropharmacology and Neurotoxicology, Shanghai University, Shanghai 200444, China*
[2]*Xinhua Translational Institute for Cancer Pain, Chongming, Shanghai 202151, China*

Abstract: Objective In this study, the pharmacological kinetics of *Buthus martensi* Karsch (BmK) AS, a specific modulator of voltage-gated sodium channel site 4, was investigated on $Na_v1.3$ expressed in *Xenopus* oocytes. **Methods** Two-electrode voltage clamp was used to record the whole-cell sodium current. **Results** The peak currents of $Na_v1.3$ were depressed by BmK AS over a wide range of concentrations (10, 100, and 500 nmol/L). Most remarkably, BmK AS at 100 nmol/L hyperpolarized the voltage-dependence and increased the voltage-sensitivity of steady-state activation/inactivation. In addition, BmK AS was capable of hyperpolarizing not only the fast inactivation but also the slow inactivation, with a greater preference for the latter. Moreover, BmK AS accelerated the time constant and increased the ratio of recovery in $Na_v1.3$ at all concentrations. **Conclusion** This study provides direct evidence that BmK AS facilitates steady-state activation and inhibits slow inactivation by stabilizing both the closed and open states of the $Na_v1.3$ channel, which might result from an integrative binding to two receptor sites on the voltage-gated sodium channels. These results may shed light on therapeutics against $Na_v1.3$-targeted pathology.

Keywords: VGSC subtype; $Na_v1.3$; VGSC site 4-specific modulator; BmK AS

1 Introduction

Aberrant expression of voltage-gated sodium channels (VGSCs) underlies the hyperexcitability of neurons and severe neuropathological syndromes. VGSCs are transmembrane proteins responsible for the initiation and conduction of action potentials along axons. The electrical activity of neurons, however, has diverse functions, such as generating repetitive firing by weak stimuli[1], amplifying subthreshold membrane potential oscillations[2-4], and conducting action potentials with high fidelity in all excitable cells[5]. To date, it has been demonstrated that the diversity of electrophysiological activities is contingent upon different VGSC subtypes ($Na_v1.1$–1.9) widely distributed in various tissues[6,7]. Although it is well-known that each VGSC subtype contributes unequally to distinct neuronal activities, the molecular mechanisms underlying this functional diversity have yet to be fully worked out.

$Na_v1.3$, a rapidly-repriming VGSC subtype only abundantly expressed in the embryonic and neonatal rodent central nervous system (CNS) and almost undetectable in the adult rodent CNS, has been implicated in inflammatory pain and epilepsy. However, the pathogenicity of $Na_v1.3$ seems to be rather obscure[8-11]. The level of $Na_v1.3$ expression

[#]Present address: School of Pharmacology, Shanghai Jiao Tong University, Shanghai 200240, China
Corresponding author: Yong-Hua Ji
Tel/Fax: +86-21-66135189
E-mail: yhji@staff.shu.edu.cn
Article ID: 1673-7067(2012)03-0209-13
Received date: 2011-12-11; Accepted date: 2012-01-27

increases in sensory neurons after transection[12-14]. Following spinal cord contusion injury, thalamic neurons undergo electrophysiological changes which are linked to the aberrant expression of $Na_v1.3$[15-17]. In dorsal root ganglion (DRG) A-fiber neurons, the mRNA of $Na_v1.3$ is up-regulated after spinal nerve ligation[18]. More notably, recent studies have revealed that $Na_v1.3$ and its auxiliary subunit β1 are both up-regulated in the hippocampus of spontaneously epileptic rats, in which a point mutation (K354Q) within the $Na_v1.3$ gene motif may contribute to the abnormal neuronal firing in hippocampal neurons[19-21]. Therefore, genetic abnormalities and aberrant electrophysiological properties of $Na_v1.3$ are likely to contribute to neuronal hyperexcitability in both the peripheral and central nervous systems. Despite these findings, the pathogenicity of $Na_v1.3$ remains unclear with regard to different expression environments *in vivo* due particularly to the scarcity of subtype-specific probes.

Long-chain neurotoxic polypeptides from *Buthus martensi* Karsch (BmK), a scorpion distributed in North China, have been reported to be specific modulators of VGSCs, either by slowing the inactivation process or by lowering the threshold for activation[22-25]. Among them, BmK AS, acting on receptor site 4 on VGSCs, were found to relief inflammatory pain responses and epileptic behavior in animal models[26-29]. By using electrophysiological recordings, such anti-nociceptive and anticonvulsant activities of BmK AS have been attributed to inhibition of the Na^+ currents through VGSCs expressed in sensory neurons[25,29,30]. Interestingly, BmK AS can even induce an opposite modulation of the peak currents of VGSCs by elevating $[Na^+]_i$ in the B104 cell line[31]. More puzzling instances have also been reported in the VGSCs endogenously expressed in the DRG neuroblastoma ND7-23 cell line and in the heterologously expressed $Na_v1.2$ in *Xenopus* oocytes, both of which exhibit a U-shaped modulation of gating kinetics by BmK AS over a wide range of concentrations[25].

To clarify the pharmacological role of BmK AS in hyperexcitability and the possible mechanisms underlying $Na_v1.3$-based pathology, we conducted a systematic investigation of the effects of BmK AS on $Na_v1.3$ expressed in *Xenopus* oocytes.

2 Materials and methods

2.1 Materials pNa3T plasmids in combination with cDNAs encoding the rat sodium channel α-subunit $rNa_v1.3α$ were kind gifts from Dr. Alan L. Goldin (University of California, Irvine, USA). BmK AS was purified by column chromatography[32] from crude venom of the Asian scorpion *B. martensi* Karsch as described previously[33]. Tetrodotoxin (TTX) (Sigma, St. Louis, MO, USA) was dissolved in stock solution (1 mmol/L TTX in 0.01% BSA solution), and diluted to 500 nmol/L with ND96 solution.

Female *Xenopus laevis* frogs were provided by the Animal Center of Shanghai Institute of Neuroscience. Oocytes were surgically removed from adult female frogs and were incubated with collagenase (2 mg/mL, type IA; Sigma) in calcium-free OR2 medium (in mmol/L: NaCl 96, KCl 2, $MgCl_2$ 1, and HEPES 5, pH 7.5) at 20°C for about 2 h. After washing, healthy oocytes at stages V–VI were selected for cRNA injection.

2.2 VGSC expression and electrophysiological studies cRNA transcripts of $rNa_v1.3$ were synthesized from Not I (TAKARA, Japan) linearized DNA templates individually using a T7 RNA-polymerase mMESSAGE mMACHINETM transcription kit (Ambion, Austin, TX, USA). *Xenopus laevis* oocytes were prepared[34,35], injected with 0.5–10 ng cRNA of $rNa_v1.3$, and incubated at 18–20°C for 2–4 days[36] in ND96 solution (containing in mmol/L: NaCl 96, KCl 2, $CaCl_2$ 1.8, $MgCl_2$ 2 and HEPES 5, pH 7.5) supplemented with 5 mmol/L pyruvate and 0.1 mg/mL gentamicin.

Two-electrode voltage-clamp recordings were performed at room temperature (18–22°C) using a Turbo TEC-03X amplifier (NPI Electronic Instruments, Germany) and Cellwork E 5.5 software (NPI). Recording electrodes were filled with 3 mol/L KCl. Currents were filtered at 1.3 kHz and sampled at 10 kHz. The composition of the bath solution was (in mmol/L): NaCl 96, KCl 2, $CaCl_2$ 1.8, $MgCl_2$ 2 and HEPES 5 (pH 7.4). BmK AS was diluted in bath solution and applied directly to the bath at the desired concentration (10, 100, or 500 nmol/L).

2.3 Data analysis Data were acquired by Cellworks Reader 3.6 (NPI) and analyzed with Origin 7.5 software (OriginLab Corp., Northampton, MA, USA).

Mean conductance (G) was calculated from peak current/voltage relations using the equation $G = I/(V-V_r)$, where I is the peak current elicited upon depolarization, V is the membrane potential, and V_r is the reversal potential. The voltage-dependence of the activation was fit with the Boltzmann relation, $G/G_{max}=1/[1+\exp(V-V_m)/k_m]$, where V_m is the voltage for half-maximum activation and k_m is the slope factor.

The voltage-dependence of fast inactivation and slow inactivation data were described with the two-state Boltzmann equation, $I/I_{max}=1/[1+\exp(V-V_{1/2})/k]$, where V is the membrane potential of the conditioning step, $V_{1/2}$ is the membrane potential at which half-maximal inactivation is achieved, and k is the slope factor. The parameters for fast inactivation were characterized by the half-maximal voltage V_f and the slope factor k_f; and those for slow inactivation by V_s and k_s, correspondingly.

Recovery data were fitted with a single exponential equation of the form $I/I_{peak} = 1\text{-}A\times\exp(-t/\tau_{rec})$, where A is the relative proportion of current recovering with time constant τ_{rec}, and t is the recovery interval.

Leak subtraction and capacitive compensation were performed by subtracting comparable records obtained in the presence of 500 nmol/L TTX. Only recordings with leakage below 0.08 μA and fluctuation within 0.05 μA were selected for statistical analysis. Data are presented as mean ± SEM. The statistical significance of differences between the parameters of currents measured in control and toxin-containing solutions was assessed with Student's two-tailed paired t test.

3 Results

3.1 Functional analysis and nonlinear dose-effect modulation of activation by BmK AS To characterize the activation kinetics of $rNa_v1.3$ by BmK AS, oocytes expressing $rNa_v1.3$ were clamped at a holding potential of -100 mV for 200 ms prior to application of a series of step stimuli.

Previous work showed that 500 nmol/L BmK AS is sufficient to induce a hyperpolarizing shift in voltage-dependent activation[25]. Therefore, 500 nmol/L BmK AS was chosen as the starting dose for all the following protocols to assess the responses of $rNa_v1.3$.

Na^+ currents were evoked by a train of depolarizations ranging from -100 mV to +70 mV at 10 mV increments, each lasting 100 ms (Fig.1A, B). Typical $rNa_v1.3$ traces were recorded in the absence and presence of 500 nmol/L BmK AS. Calculating the percentage of peak current normalized to that of control showed that the peak currents of $rNa_v1.3$ were remarkably inhibited to about 80% of control after perfusion with 500 nmol/L BmK AS for 20 min (Fig. 1E, Fig. 2). The inhibition of I_{peak} by BmK AS could not be reversed to the control level even when the washing duration was extended for up to 30 min (Fig. 1F). Oocytes exposed to 100 nmol/L BmK AS (inhibited to about 50% of control) had a greater response than those with 10 nmol/L (inhibited to about 80% of control, Fig.1C) and 500 nmol/L BmK AS (inhibited to about 80% of control) (Fig. 1D and Fig. 2).

Unlike the less potent inhibition of I_{peak}, 10 nmol/L BmK AS induced the greatest shift in voltage-dependent activation ($V_{1/2}$) toward a more negative potential by 9.18 ± 0.97 mV (P <0.001, n = 12), while $V_{1/2}$ was shifted by 5.34 ± 0.71 mV at 100 nmol/L (n = 14) and even less (4.08 ± 0.08 mV, n = 19) at 500 nmol/L (Fig. 3, Table 1). Notably, the hyperpolarizing shift of activation by 500 nmol/L BmK AS could be relieved after a 10 min period of washing (data not shown). In addition, the slope factor (k) of the activation curve, indicating the range of voltage sensitivity, was slightly increased by BmK AS (1.55 mV for 10 nmol/L, 1.27 mV for 100 nmol/L and 2.04 mV for 500 nmol/L) (Table 1). As the inhibition of peak currents and the shift in voltage-dependent activation of $rNa_v1.3$ by BmK AS were inconsistent with the low-to-high concentrations administered, $Na_v1.3$ activation may be modulated by BmK AS in a nonlinear manner.

3.2 Nonlinear dose-effect modulation of steady-state inactivation by BmK AS For steady-state inactivation, $rNa_v1.3$ expressed in oocytes underwent a series of depo-

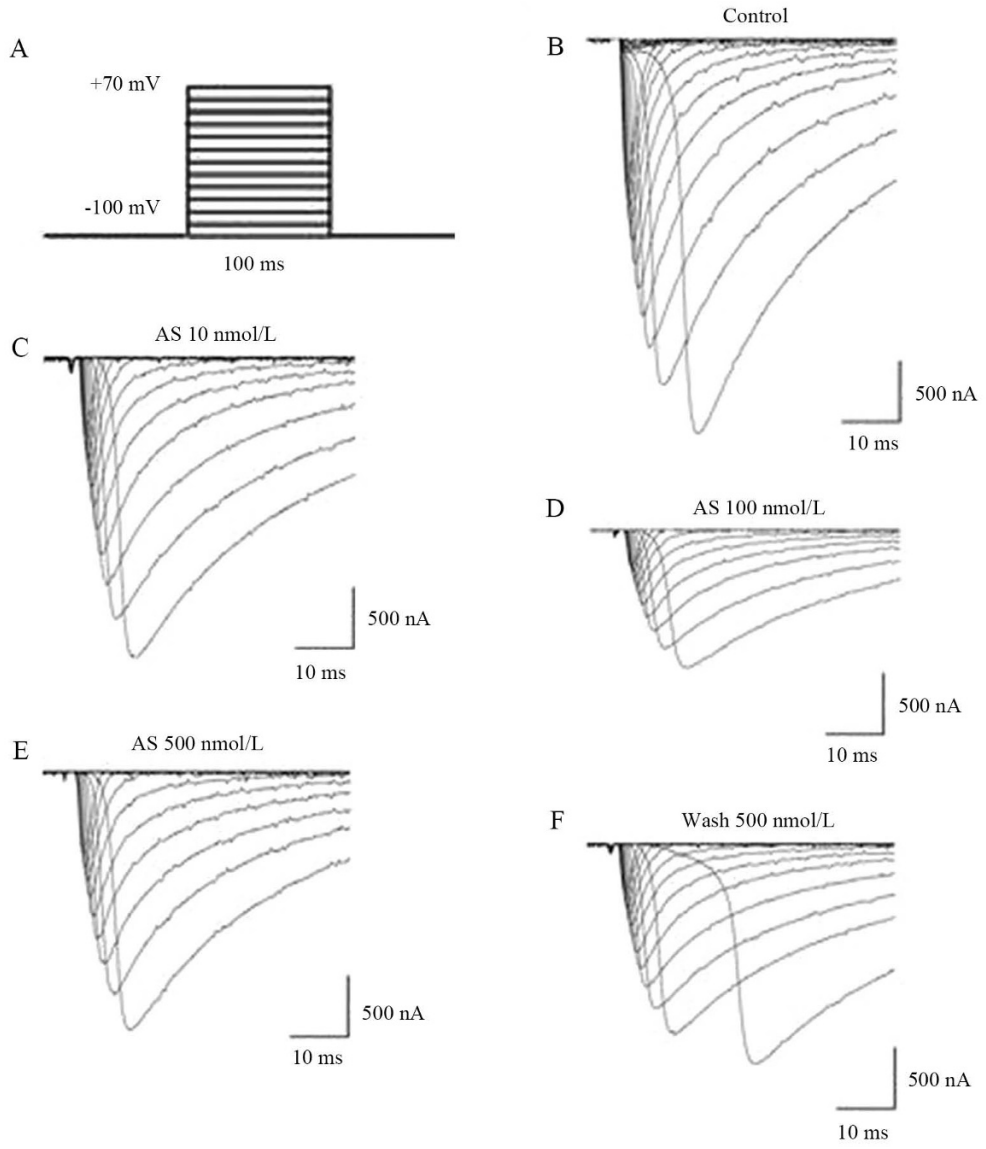

Fig. 1. Effects of BmK AS on peak currents of rNa$_v$1.3. A: Stimulus protocol for channel activation. B–E: Na^+ current traces elicited during long-lasting step depolarizations from -100 mV to +70 mV in the absence or presence of BmK AS at 10, 100 and 500 nmol/L. F: Failure to washout effects of 500 nmol/L BmK AS for 10 min.

larizing prepulses ranging from -100 mV to +40 mV for up to 500 ms and was assessed as the amplitude remaining at a test potential of -10 mV immediately after each prepulse (Fig. 4 inset).

After perfusion of each concentration of BmK AS for 20 min independently, the normalized decaying currents of rNa$_v$1.3 were all shifted to hyperpolarized potentials to different extents. The inactivation kinetics were altered more by 100 nmol/L BmK AS than by 10 and 500 nmol/L (Fig. 4). Compared to the control, 100 nmol/L BmK AS shifted the $V_{1/2}$ by 18.44 ± 0.53 mV (P <0.001, n = 13), while the $V_{1/2}$ was shifted by 13.80 ± 0.05 mV (P <0.001, n = 8) with 10 nmol/L and 7.35 ± 0.18 mV (n = 21) with 500 nmol/L (Table 1). Contrary to the comparatively weak binding affinity with rNa$_v$1.3 in the activation process at high concentration, BmK AS at all concentrations was hardly dis-

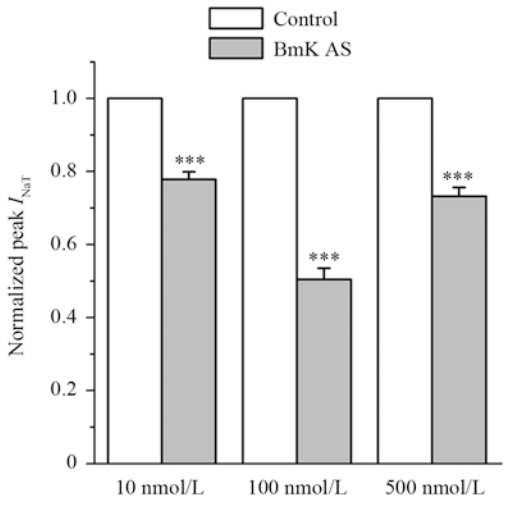

Fig. 2. Normalized transient Na^+ peak current (peak I_{NaT}) before (control, open bars) and after BmK AS administration. ***P <0.001.

sociated in the steady-state inactivation process. Still, the slope factor (k) of the inactivation curves of $rNa_v1.3$ was also slightly increased by BmK AS (0.74 mV for 10 nmol/L, 3.96 mV for 100 nmol/L and 3.14 mV (P <0.001) for 500 nmol/L), similar to that in the activation process (Table 1). Therefore, the steady-state inactivation of $rNa_v1.3$ was also modulated by BmK AS in a nonlinear manner.

3.3 Nonlinear dose-effect modulation of open- and closed-state inactivation by BmK AS Since BmK AS had a comparatively potent preference for steady-state inactivation over voltage-dependent activation, we investigated the effects of BmK AS on the fast and slow inactivation kinetics of $rNa_v1.3$.

The voltage-dependence of fast and slow inactivation was studied using prepulses of different durations (10 ms

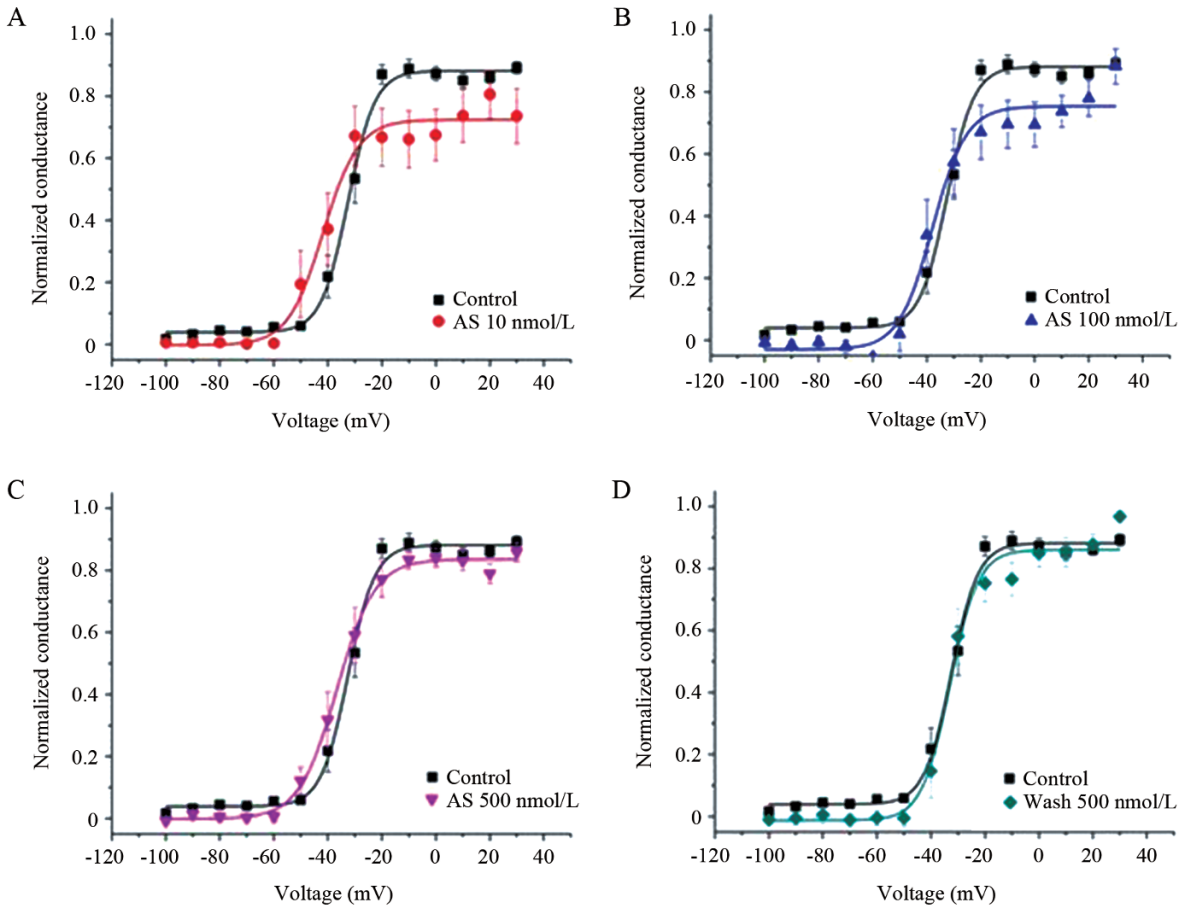

Fig. 3. Effects of different concentrations of BmK AS on voltage-dependent activation of $rNa_v1.3$ (A–C) and effect of washout at 500 nmol/L (D) for 10 min.

Table 1. Electrophysiological parameters of rNav1.3 modulated by BmK AS

Concentration	Steady-state activation		
	$V_{1/2}$ (mV)	k	n
Control	-32.54±0.53	4.95±0.46	26
AS 10 nmol/L	-41.72±1.51***	6.50±1.32	12
AS 100 nmol/L	-37.88±1.25	6.22±1.09	14
AS 500 nmol/L	-36.62±0.63	6.70±0.55***	19
Wash	-32.98±0.86	5.20±0.74	14
		Steady-state inactivation	
Control	-34.96±0.60	6.8885±0.52	22
AS 10 nmol/L	-48.76±0.55***	7.6309±0.48	8
AS 100 nmol/L	-53.39±1.21***	10.84±1.05***	13
AS 500 nmol/L	-42.30±0.79	10.03±0.70***	21
Wash	-40.63±0.88	8.48±0.78	15
		Fast inactivation	
Control	-38.05±0.82	7.29±0.71	10
AS 10 nmol/L	-46.31±0.91***	7.98±0.80	9
AS 100 nmol/L	-40.47±0.95	8.55±0.83	12
AS 500 nmol/L	-47.86±1.12***	8.74±0.98	10
Wash	-38.88±0.91	4.82±0.84	8
		Slow inactivation	
Control	-32.66±0.52	4.03±0.44	10
AS 10 nmol/L	-42.98±0.98***	7.70±0.86***	9
AS 100 nmol/L	-49.77±1.27***	10.92±1.13***	10
AS 500 nmol/L	-46.13±0.87***	9.66±0.77***	10
Wash	-35.75±0.83	6.66±0.72	8
		Recovery	
	A	τ_{rec} (ms)	n
Control	0.97±0.00	4.02±0.15	12
AS 10 nmol/L	0.98±0.00***	2.22±0.06***	7
AS 100 nmol/L	0.98±0.00***	1.85±0.05***	9
AS 500 nmol/L	0.99±0.00***	2.00±0.06***	7
Wash	0.98±0.00	2.31±0.03***	7

For voltage-dependent activation/inactivation, the values of half-maximum activation/inactivation voltage $V_{1/2}$ and corresponding slope factor (k) were determined in the absence and presence of BmK AS. For recovery, total recovery of sodium channels is indicated as A and τ_{rec} is the time constant of recovery. The data are mean ± SEM and n is the number of independent experiments. ***P <0.001 *vs* control.

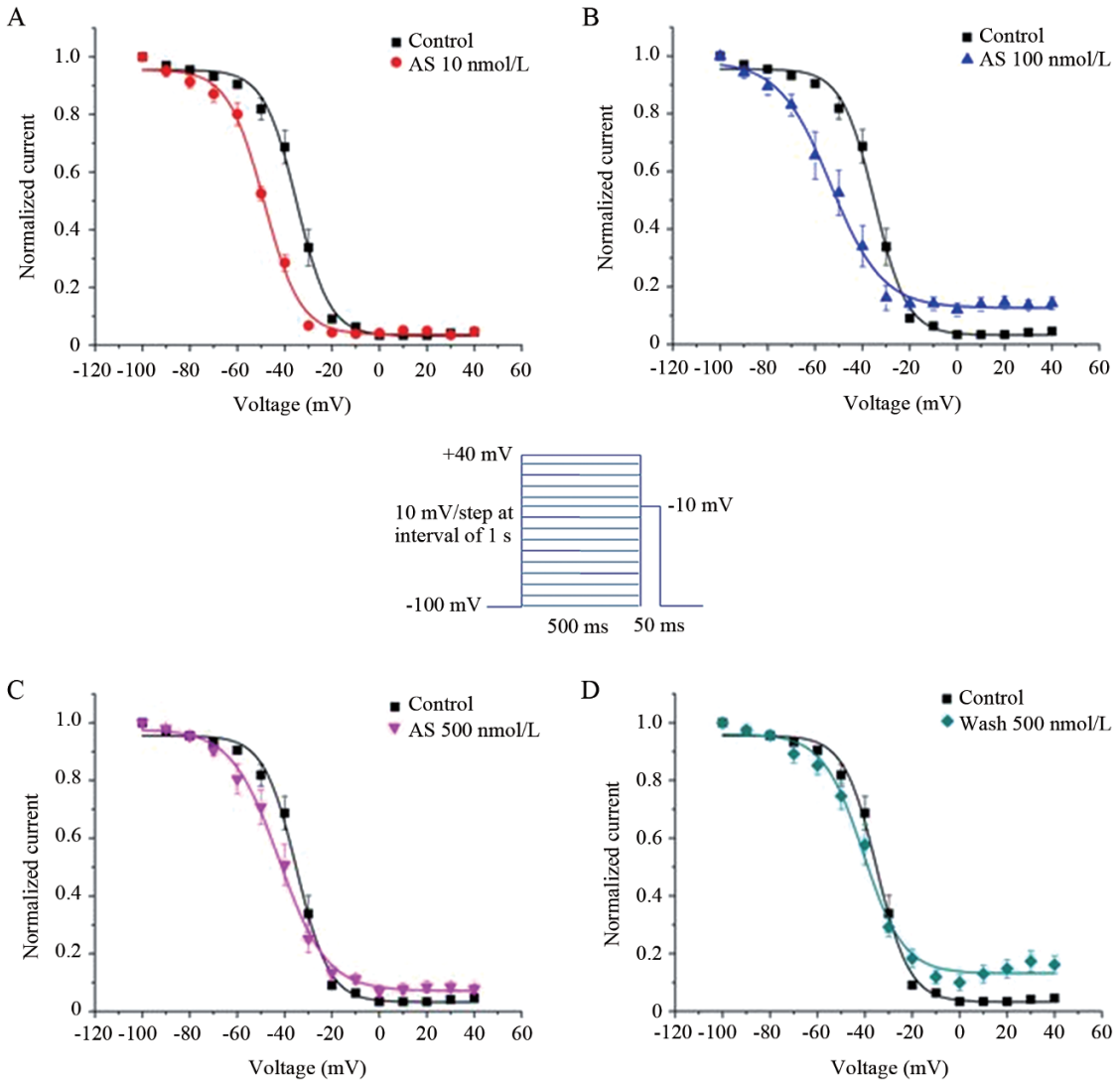

Fig. 4. Effects of different concentrations of BmK AS on steady-state inactivation of rNa$_v$1.3 (A–C) and washout of 500 mmol/L (D) for 10 min. Inset shows the protocol for steady-state inactivation.

for fast and 2 s for slow inactivation) (insets in Fig. 5).

Both 10 and 500 nmol/L BmK AS had a significant effect on fast inactivation, shifting the half-maximum inactivation potential more negative ($V_{1/2}$) by 8.26 ± 0.09 mV (P <0.001, n = 9) and 9.82 ± 0.31 mV (P <0.001, n = 10) respectively. Unexpectedly, 100 nmol/L BmK AS hardly shifted the voltage-dependent fast inactivation. The change of slope factor of fast inactivation was less than that of the steady-state inactivation and activation processes, increased by 0.69 mV for 10 nmol/L (P <0.001, n = 9), 1.26 mV for 100 nmol/L (P <0.001, n = 12) and 1.45 mV for 500 nmol/L (P <0.001, n = 10) (Fig. 5, Table 1). However, k was remarkably decreased by 2.46 mV after washing, compared to the control, indicating an expansion in voltage-sensitivity during the administration (Table 1).

In the case of slow inactivation, BmK AS shifted the voltage-dependent inactivation kinetics towards more negative vlaues at all concentrations. Contrary to the insensitivity of fast inactivation kinetics to 100 nmol/L BmK AS, $V_{1/2}$ exhibited a most remarkable negative shift by 17.10 ± 0.75 mV at this concentration (P <0.001, n = 10). In the presence of 10 or 500 nmol/L BmK AS, the values of $V_{1/2}$ were

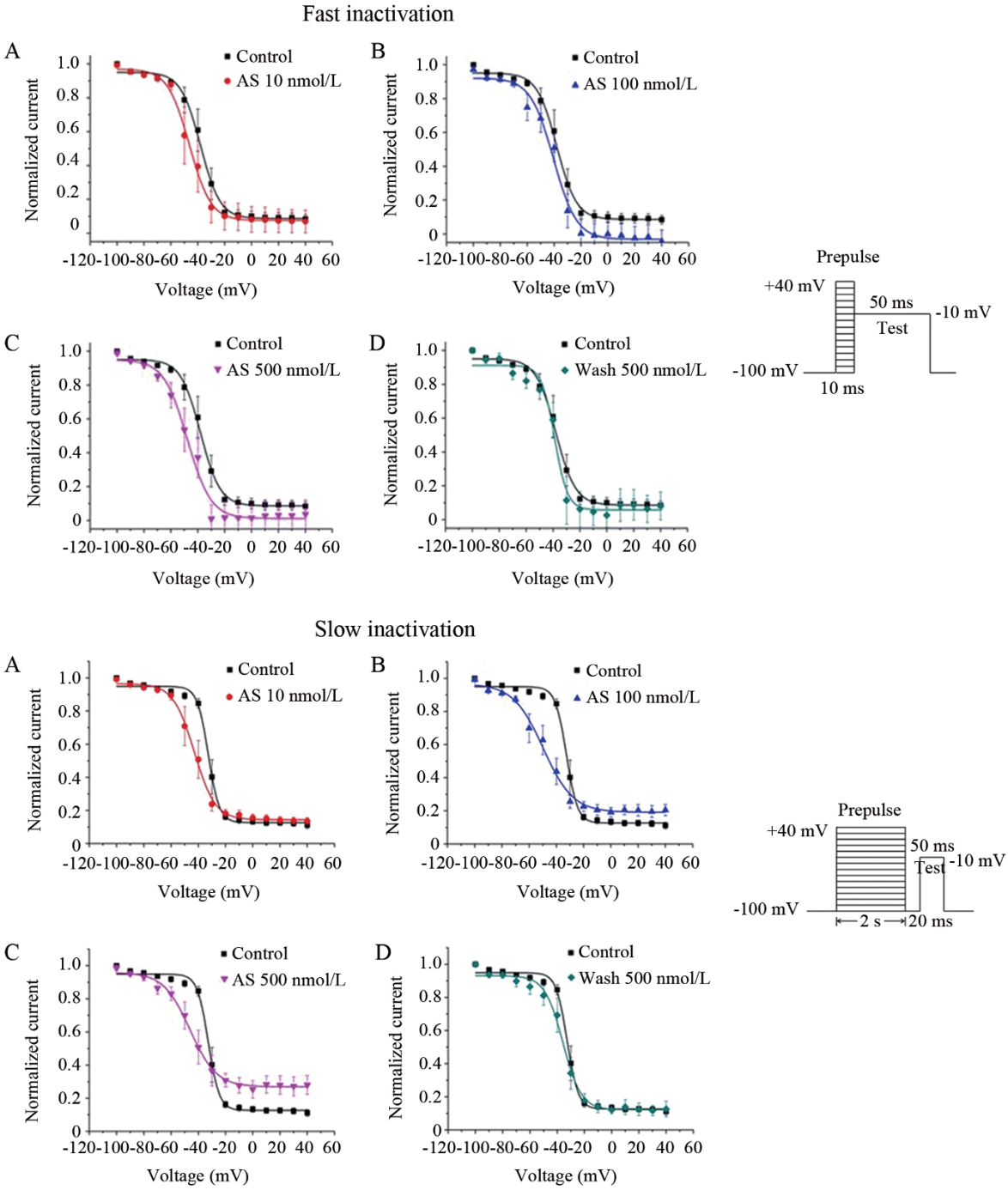

Fig. 5. Effects of different concentrations of BmK AS on voltage-dependent fast (upper panels, A-C) and slow (lower panels, A-C) inactivation of rNa$_v$1.3. Effects of washout for 10 min after 500 nmol/L in D for each. Right hand insets show the stimulation protocols.

also greatly hyperpolarized, negatively shifted by 10.31 ± 0.47 mV (P <0.001, n = 9) and 13.46 ± 0.36 mV (P < 0.001, n = 10), respectively (Fig. 5, Table 1). Despite the pronounced change in slow inactivation kinetics, the hyperpolarized $V_{1/2}$ almost returned to the control level after washing, except for k that still had a significant negative

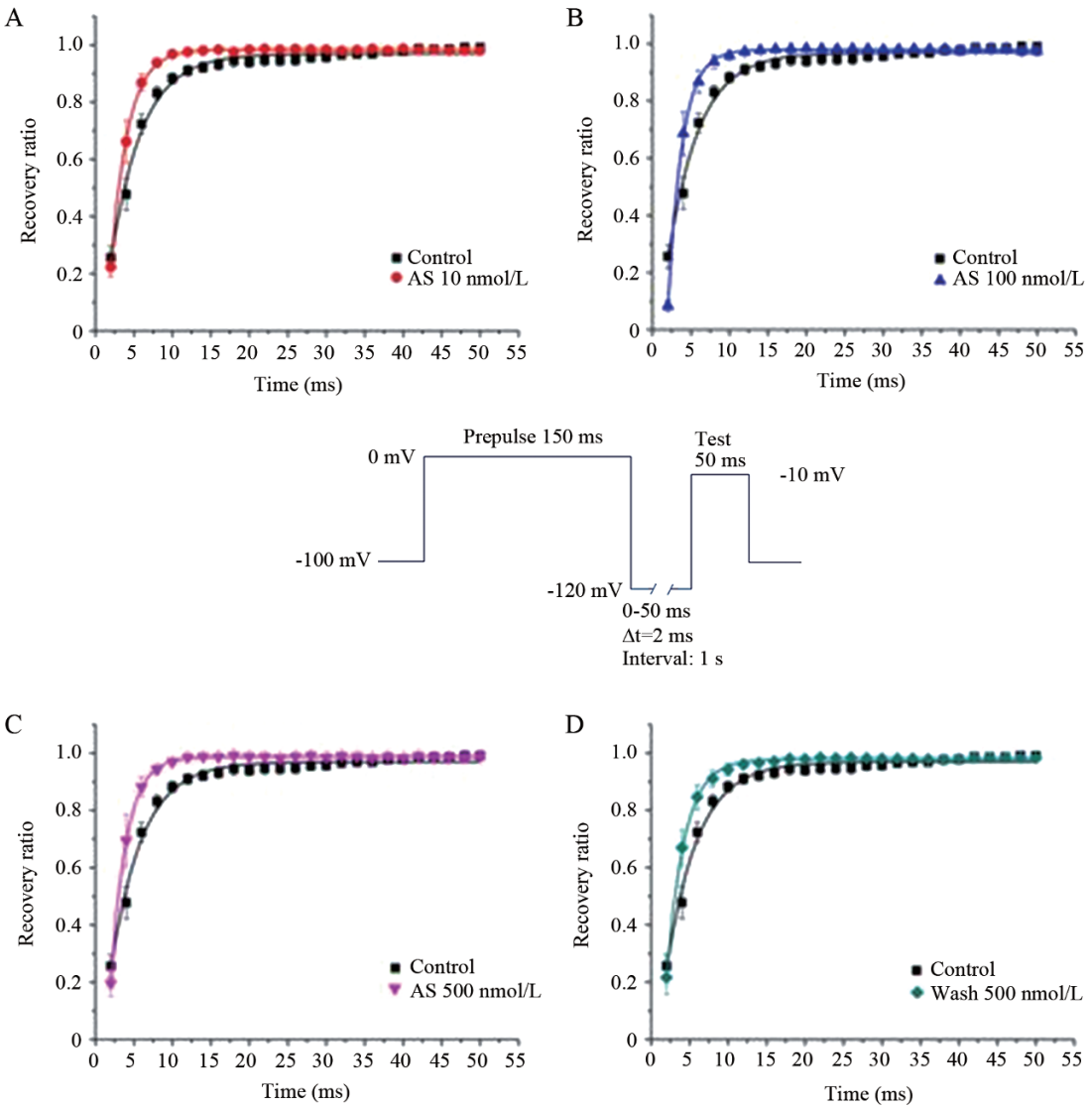

Fig. 6. Effects of different concentrations of BmK AS on time course of $rNa_v1.3$ recovery (A–C) and effect of washout from 500 nmol/L for 10 min (D). Inset shows the protocol for rNa1.3 recovery test.

enhancement [increased by 3.64 mV for 10 nmol/L ($P < 0.001$, $n = 9$), 6.89 mV for 100 nmol/L ($P < 0.001$, $n = 10$) and 5.63 mV for 500 nmol/L ($P < 0.001$, $n = 10$)] (Table 1).

Thus, BmK AS modulated both fast and slow inactivation of $rNa_v1.3$ in a nonlinear manner, with more effect on slow inactivation.

3.4 Nonlinear dose-effect acceleration of recovery from BmK AS To correlate the inactivation and recovery from inactivation of $rNa_v1.3$ in the presence of BmK AS, the recovery kinetics of currents were measured at a recovery voltage of -120 mV and single exponential fits were used to estimate the recovery time constants.

The rate of recovery was accelerated to variable extents by different doses of BmK AS. The acceleration of recovery kinetics from 100 nmol/L BmK AS was the most notable ($\Delta\tau_{rec} = 2.17 \pm 0.10$ ms, $n = 9$), while 10 and 500 nmol/L were less efficient ($\Delta\tau_{rec} = 1.81 \pm 0.09$ ms, $n = 7$ and $\Delta\tau_{rec} = 2.02 \pm 0.09$ ms, $n = 7$) (Fig. 6, Table 1). At all concentrations, BmK AS shifted the voltage-dependence of recovery in the hyperpolarized direction (Fig. 6), leading to

a slight enhancement of total recovery of $rNa_v1.3$ at -120 mV. However, this enhancement was comparatively less remarkable for 100 nmol/L BmK AS (increased by 1.03%, P <0.001) than that for 10 nmol/L (increased by 1.43%, P <0.001) and 500 nmol/L (increased by 1.79%, P <0.001) (Table 1). These results suggested that BmK AS accelerated the recovery of $rNa_v1.3$ from inactivation in a nonlinear manner.

4 Discussion

4.1 Nonlinear dose-effect modulation of activation and inactivation of $rNa_v1.3$ by BmK AS The $Na_v1.3$ channel is the only VGSC subtype that has up-regulated expression in injured neurons[12-14,17,18]. $Na_v1.3$ currents exhibit slow development of closed-state inactivation and rapid repriming kinetics in response to depolarizing stimuli[37]. The distinct functional properties of $Na_v1.3$ may be important for developing neurons and also contribute to aberrant activity in injured neurons.

In the present study, we expressed the $rNa_v1.3$ α subunit alone in *Xenopus* oocytes to specifically investigate the pharmacology of BmK AS, a VGSC site 4-specific modulator, on $Na_v1.3$. The fact that the electrophysiological profiles of one type of channel may vary in different expression systems does not affect our goal to assess the pharmacological modulation of $Na_v1.3$ by BmK AS. Indeed, our data demonstrated a more negative shift in activation by -10 mV than a previous report which also used *Xenopus* oocytes[21], and this is close to the value expressed in HEK 293 cells[37]. However, the shift in inactivation kinetics appeared to be more profoundly depolarized than that of $Na_v1.3$ expressed in HEK 23 cells or axotomized DRG neurons[37]. The subtle variances may be attributed the comparatively longer time of channel expression required to ensure robust currents, which did not influence the following studies. Another possibility may lie in the lack of β subunits, which has been demonstrated to result in a similar functional contrast[21,38].

The nonlinear dose-effect curve for BmK AS was first assessed on $Na_v1.2$ expressed in *Xenopus* oocytes and ND7-23 cells. For $Na_v1.2$, BmK AS was found to depolarize the voltage-dependent activation and inactivation at low (0.1 nmol/L) and high concentrations, but hyperpolarize the activation and inactivation kinetics at a medium concentration (1 nmol/L)[25]. Interestingly, in ND7-23 cells that express a mixture of TTX-sensitive VGSCs, mainly $Na_v1.6$ and $Na_v1.7$[39], BmK AS hyperpolarizes the voltage-dependence of activation and inactivation at 0.1, 1 and 100 nmol/L but not at 10 nmol/L. However, in the present study, BmK AS hyperpolarized the voltage-dependence of activation and inactivation at all three concentrations, resembling its actions on ND 7-23 cells but unlike those on $Na_v1.2$. The ability of BmK AS to hyperpolarize the channel activation/inactivation process may reflect a facilitation of the threshold for channel opening and repetitive firing, which may lead to hyperexcitability. One interesting finding of this study was that the modulatory direction of voltage-dependence of activation and inactivation by BmK AS between $Na_v1.3$ and $Na_v1.2$ appear to be opposing, which could be explained by subtle structural or static environmental variations in the toxin-binding site between the two channels. Accordingly, the similar potency of BmK AS for $Na_v1.3$ and ND7-23 cells leads to the speculation that the binding sites of $Na_v1.3$ are more homologous to those of $Na_v1.6$/$Na_v1.7$, although supportive clues at the molecular level remain to be approached.

4.2 Possible mechanism of BmK AS interaction with $Na_v1.3$ From the current results, BmK AS facilitated both the voltage-dependent activation and inactivation of $Na_v1.3$ over a wide range of concentrations (i.e., 10, 100 and 500 nmol/L). This dual potency seems to be a common feature among other known β-like toxins that are toxic to both mammal and insects, such as BmK AS-1, AaH IT4 and Lqhβ1[40].

Like AaH IT4, BmK AS/AS-1 competes with anti-insect scorpion toxins for binding to the sodium channel of insects at a site with high affinity but low capacity; it also competes with the binding of α-type scorpion toxins to the mammalian sodium channel at a low affinity but high capacity binding site[41,43]. Generally, α-type scorpion toxins, defined as VGSC site 3-specific modulators, target VGSCs by inhibiting the inactivation and recovery, while β-type

anti-insect scorpion toxins, defined as VGSC site 4-specific modulators, facilitate the activation and depress the peak currents of VGSCs[44,45]. Hence, it is reasonable to assume that BmK AS can bind to both sites 3 and 4, modulating both voltage-dependent activation and inactivation of VGSCs. BmK AS tended to bind with site 3 to modulate inactivation more at the medium concentration, while binding with site 4 at low or high concentrations caused more of a negative-shift of the activation. In terms of these multifaceted features, BmK AS resembles another β-like toxin, Lqhβ1, which induces a shift in the voltage-dependent activation to more negative membrane potentials and a reduction in peak sodium currents, as well as having a weak effect on inactivation of cardiac VGSCs and a marked effect on rat brain and skeletal muscle VGSCs[40].

It is noteworthy that BmK AS had a comparably stronger modulation of inactivation than activation, which was inferred by the finding that the shift in voltage-dependent inactivation by BmK AS was far more difficult to remove by washing compared to the almost full recovery of BmK AS-modified voltage-dependent activation. Therefore, the tight binding of BmK AS with the inactivation gate of the channel may result in a shift in recovery kinetics and an overall reduction in peak currents even after washing. Considering the fact that site 4-specific modulators facilitate activation by binding to the DII S3/S4 loop in VGSCs[46] while site 3-specific modulators delay inactivation by binding to DIV S4[43], we may infer that BmK AS binds with the DII S3/S4 loop and DIV S4 in particular. More supportive evidence came from the finding that the slow inactivation kinetics were more readily modulated than the fast inactivation by BmK AS, in that the molecular determinants of slow inactivation are considered to be more closely associated with the charged residues within DIV S4[47]. However, this inference should be interpreted with caution until more evidence from molecular site-directed mutagenesis is available.

4.3 Pathogenetic insights into $Na_v1.3$ probed by BmK AS It has been shown that spinal contusion leads to a shift of the steady-state activation and inactivation of the sodium current towards more depolarized potentials. The shifted steady-state inactivation shows similarities to that in axotomized DRGs, which is attributed to upregulated $Na_v1.3$ expression[16,17]. These observations imply a substantial involvement of $Na_v1.3$ in pathogenesis by depolarizing the membrane potential. Accordingly, in the present study, BmK AS potently shifted the voltage-dependent activation/inactivation of $Na_v1.3$ in the hyperpolarized direction. Although this hyperpolarized shift may not be predominant at low or high concentrations, partly due to the integral interaction of sites 3 or 4 with BmK AS, it is clear that BmK AS has potential value as a modulator in inflammatory pain studies.

A marked finding of this study was that BmK AS inhibited the peak current of $Na_v1.3$ at all concentrations tested. The inhibition of Na^+ currents is in accord with the previous experiments on pathology, i.e., the nociceptive responses induced by formalin or carrageenan are markedly reduced after BmK AS administration[26-28]. Accordingly, the seizure-like behavior and cortical epileptiform EEG in epileptic rats are remarkably suppressed by BmK AS[29]. However, this anti-convulsant activity of BmK AS seems to differ among epileptic models, being efficient in pentylenetetrazole-evoked seizures but ineffective in pilocarpine-induced epileptiform behavior[29]. The relative strength of the opposing effects may depend on the toxin concentration and the VGSC subtypes affected[25].

Although the inhibition of Na^+ current by BmK AS is apparent in heterologously expressed VGSCs, the intracellular Na^+ concentration is unexpectedly elevated by 500 nmol/L BmK AS in the B104 neuroblastoma cell line[48], in which $Na_v1.3$ and $Na_v1.6$ are dominantly expressed[49]. The hyperpolarized threshold may trigger an increase in $[Na^+]_i$ and membrane depolarization, which could in turn initiate downstream protein-coupled signaling pathways, activating ion channels or transporters. Hence, the modulation of $[Na^+]_i$ by BmK AS may affect the physiological function of cells, and thereby provide insights into VGSC-mediated disorders.

Acknowledgements: This work was supported by grants from the National Basic Research Development

Program of China (2010CB529806), the National Natural Science Foundation of China (31171064), the Key Research Program of Science and Technology Commissions of Shanghai Municipality (11JC1404300) and the Leading Academic Discipline Project of Shanghai Municipal Education Commission (J50108).

References:

[1] Franceschetti S, Guatteo E, Panzica F, Sancini G, Wanke E, Avanzini G. Ionic mechanisms underlying burst firing in pyramidal neurons: intracellular study in rat sensorimotor cortex. Brain Res 1995, 696: 127–139.

[2] Alonso A, Llinas RR. Subthreshold Na^+-dependent theta-like rhythmicity in stellate cells of entorhinal cortex layer II. Nature 1989, 342: 175–177.

[3] Klink R, Alonso A. Ionic mechanisms for the subthreshold oscillations and differential electroresponsiveness of medial entorhinal cortex layer II neurons. J Neurophysiol 1993, 70: 144–157.

[4] Silva LR, Amitai Y, Connors BW. Intrinsic oscillations of neocortex generated by layer 5 pyramidal neurons. Science 1991, 251: 432–435.

[5] Crill WE. Persistent sodium current in mammalian central neurons. Annu Rev Physiol 1996, 58: 349–362.

[6] Catterall WA. Cellular and molecular biology of voltage-gated sodium channels. Physiol Rev 1992, 72: S15–48.

[7] Catterall WA. Structure and function of voltage-gated ion channels. Annu Rev Biochem 1995, 64: 493–531.

[8] Beckh S, Noda M, Lubbert H, Numa S. Differential regulation of three sodium channel messenger RNAs in the rat central nervous system during development. EMBO J 1989, 8: 3611–3616.

[9] Black JA, Waxman SG. Sodium channel expression: a dynamic process in neurons and non-neuronal cells. Dev Neurosci 1996, 18: 139–152.

[10] Felts PA, Yokoyama S, Dib-Hajj S, Black JA, Waxman SG. Sodium channel alpha-subunit mRNAs I, II, III, NaG, Na6 and hNE (PN1): different expression patterns in developing rat nervous system. Brain Res Mol Brain Res 1997, 45: 71–82.

[11] Holland KD, Kearney JA, Glauser TA, Buck G, Keddache M, Blankston JR, *et al*. Mutation of sodium channel SCN3A in a patient with cryptogenic pediatric partial epilepsy. Neurosci Lett 2008, 433: 65–70.

[12] Black JA, Cummins TR, Plumpton C, Chen YH, Hormuzdiar W, Clare JJ, *et al.* Upregulation of a silent sodium channel after peripheral, but not central, nerve injury in DRG neurons. J Neurophysiol 1999, 82: 2776–2785.

[13] Dib-Hajj SD, Fjell J, Cummins TR, Zheng Z, Fried K, LaMotte R, *et al.* Plasticity of sodium channel expression in DRG neurons in the chronic constriction injury model of neuropathic pain. Pain 1999, 83: 591–600.

[14] Hains BC, Saab CY, Klein JP, Craner MJ, Waxman SG. Altered sodium channel expression in second-order spinal sensory neurons contributes to pain after peripheral nerve injury. J Neurosci 2004, 24: 4832–4839.

[15] Kamata K, Kirisawa H. Changes in electrophysiological properties and noradrenaline response in vas deferens of diabetic rats. Eur J Pharmacol 1998, 350: 237–241.

[16] Hains BC, Klein JP, Saab CY, Craner MJ, Black JA, Waxman SG. Upregulation of sodium channel Nav1.3 and functional involvement in neuronal hyperexcitability associated with central neuropathic pain after spinal cord injury. J Neurosci 2003, 23: 8881–8892.

[17] Lampert A, Hains BC, Waxman SG. Upregulation of persistent and ramp sodium current in dorsal horn neurons after spinal cord injury. Exp Brain Res 2006, 174: 660–666.

[18] Kim CH, Oh Y, Chung JM, Chung K. The changes in expression of three subtypes of TTX sensitive sodium channels in sensory neurons after spinal nerve ligation. Brain Res Mol Brain Res 2001, 95: 153–161.

[19] Estacion M, Gasser A, Dib-Hajj SD, Waxman SG. A sodium channel mutation linked to epilepsy increases ramp and persistent current of Nav1.3 and induces hyperexcitability in hippocampal neurons. Exp Neurol 224: 362–368.

[20] Guo F, Yu N, Cai JQ, Quinn T, Zong ZH, Zeng YJ, *et al.* Voltage-gated sodium channel Nav1.1, Nav1.3 and beta1 subunit were upregulated in the hippocampus of spontaneously epileptic rat. Brain Res Bull 2008, 75: 179–187.

[21] Patton DE, Isom LL, Catterall WA, Goldin AL. The adult rat brain beta 1 subunit modifies activation and inactivation gating of multiple sodium channel alpha subunits. J Biol Chem 1994, 269: 17649–17655.

[22] Feng XH, Chen JX, Liu Y, Ji YH. Electrophysiological characterization of BmK I, an alpha-like scorpion toxin, on rNav1.5 expressed in HEK293t cells. Toxicol In Vitro 2008, 22: 1582–1587.

[23] He H, Liu Z, Dong B, Zhou J, Zhu H, Ji Y. Molecular determination of selectivity of the site 3 modulator (BmK I) to sodium channels in the CNS: a clue to the importance of Nav1.6 in BmK I-induced neuronal hyperexcitability. Biochem J 2010, 431: 289–298.

[24] Tan ZY, Xiao H, Mao X, Wang CY, Zhao ZQ, Ji YH. The inhibitory effects of BmK IT2, a scorpion neurotoxin on rat nociceptive flexion reflex and a possible mechanism for modulating voltage-gated Na^+ channels. Neuropharmacology 2001, 40: 352–357.

[25] Zhu MM, Tao J, Tan M, Yang HT, Ji YH. U-shaped dose-dependent effects of BmK AS, a unique scorpion polypeptide toxin, on voltage-gated sodium channels. Br J Pharmacol 2009, 159: 1895–1903.

[26] Chen B, Ji Y. Antihyperalgesia effect of BmK AS, a scorpion toxin, in rat by intraplantar injection. Brain Res 2002, 952: 322–326.

[27] Chen J, Feng XH, Shi J, Tan ZY, Bai ZT, Liu T, *et al.* The antinociceptive effect of BmK AS, a scorpion active polypeptide, and the possible mechanism on specifically modulating voltage-gated Na^+ currents in primary afferent neurons. Peptides 2006, 27: 2182–2192.

[28] Liu T, Pang XY, Jiang F, Bai ZT, Ji YH. Anti-nociceptive effects induced by intrathecal injection of BmK AS, a polypeptide from the venom of Chinese-scorpion *Buthus martensi* Karsch, in rat formalin test. J Ethnopharmacol 2008, 117: 332–338.

[29] Zhao R, Weng CC, Feng Q, Chen L, Zhang XY, Zhu HY, *et al.* Anticonvulsant activity of BmK AS, a sodium channel site 4-specific modulator. Epilepsy Behav 2011, 20: 267–276.

[30] Tan M, Zhu MM, Liu Y, Cheng HW, Ji YH. Effects of BmK AS on Nav1.2 expressed in *Xenopus laevis* oocytes. Cell Biol Toxicol 2008, 24: 143–149.

[31] Tan ZY, Chen J, Shun HY, Feng XH, Ji YH. Modulation of BmK AS, a scorpion neurotoxic polypeptide, on voltage-gated Na^+ channels in B104 neuronal cell line. Neurosci Lett 2003, 340: 123–126.

[32] Liu YR, Ren H M, Ji Y H, Ohishi T, Mochizuki T, Hoahino M, *et al*. Purification and the partial amino acid sequence of a novel activator of ryanodine (bmk as-1) from mammalian skeletal muscle. Biomed Res 1996, 17: 451–455.

[33] Ji YH, Mansuelle P, Terakawa S, Kopeyan C, Yanaihara N, Hsu K, *et al.* Two neurotoxins (BmK I and BmK II) from the venom of the scorpion *Buthus martensi* Karsch: purification, amino acid sequences and assessment of specific activity. Toxicon 1996, 34: 987–1001.

[34] Goldin AL. Expression of ion channels by injection of mRNA into *Xenopus* oocytes. Methods Cell Biol 1991, 36: 487–509.

[35] Shichor I, Zlotkin E, Ilan N, Chikashvili D, Stuhmer W, Gordon D, *et al.* Domain 2 of Drosophila para voltage-gated sodium channel confers insect properties to a rat brain channel. J Neurosci 2002, 22: 4364–4371.

[36] Smith MR, Smith RD, Plummer NW, Meisler MH, Goldin AL. Functional analysis of the mouse Scn8a sodium channel. J Neurosci 1998, 18: 6093–6102.

[37] Cummins TR, Aglieco F, Renganathan M, Herzog RI, Dib-Hajj SD, Waxman SG. Nav1.3 sodium channels: rapid repriming and slow closed-state inactivation display quantitative differences after expression in a mammalian cell line and in spinal sensory neurons. J Neurosci 2001, 21: 5952–5961.

[38] Meadows LS, Chen YH, Powell AJ, Clare JJ, Ragsdale DS. Functional modulation of human brain Nav1.3 sodium channels, expressed in mammalian cells, by auxiliary beta 1, beta 2 and beta 3 subunits. Neuroscience 2002, 114: 745–753.

[39] John VH, Main MJ, Powell AJ, Gladwell ZM, Hick C, Sidhu HS, *et al.* Heterologous expression and functional analysis of rat Nav1.8 (SNS) voltage-gated sodium channels in the dorsal root ganglion neuroblastoma cell line ND7-23. Neuropharmacology 2004, 46: 425–438.

[40] Gordon D, Ilan N, Zilberberg N, Gilles N, Urbach D, Cohen L, *et al.* An 'Old World' scorpion beta-toxin that recognizes both insect and mammalian sodium channels. Eur J Biochem 2003, 270: 2663–2670.

[41] Li YJ, Liu Y, Ji YH. BmK AS: new scorpion neurotoxin binds to distinct receptor sites of mammal and insect voltage-gated sodium channels. J Neurosci Res 2000, 61: 541–548.

[42] Jia LY, Zhang JW, Ji YH. Biosensor binding assay of BmK AS-1, a novel Na^+ channel-blocking scorpion ligand on rat brain synaptosomes. Neuroreport 1999, 10: 3359–3362.

[43] Liu ZR, Ye P, Ji YH. Exploring the obscure profiles of pharmacological binding sites on voltage-gated sodium channels by Bmk neurotoxins. Protein Cell 2011, 2: 437–444.

[44] Cestele S, Catterall WA. Molecular mechanisms of neurotoxin action on voltage-gated sodium channels. Biochimie 2000, 82: 883–892.

[45] Zuo XP, Ji YH. Molecular mechanism of scorpion neurotoxins acting on sodium channels: insight into their diverse selectivity. Mol Neurobiol 2004, 30: 265–278.

[46] de la Vega RC, Possani LD. Novel paradigms on scorpion toxins that affects the activating mechanism of sodium channels. Toxicon 2007, 49: 171–180.

[47] Ulbricht W. Sodium channel inactivation: molecular determinants and modulation. Physiol Rev 2005, 85: 1271–1301.

[48] Tan ZY, Chen J, Feng XH, Susumu T, Ji YH. Modulation of intracellular Na^+ concentration by BmK AS, a scorpion toxin, in B104 cell line. Neuroreport 2004, 15: 13–16.

[49] Oh Y, Waxman SG. Novel splice variants of the voltage-sensitive sodium channel alpha subunit. Neuroreport 1998, 9: 1267–1272.